Time-resolved photoluminescence studies of Al-rich AlGaN alloys

J. Li, K. B. Nam, T. N. Oder, K. H. Kim, M. L. Nakarmi, J. Y. Lin, and H. X. Jiang[a)]
Department of Physics, Kansas State University, Manhattan, KS 66506-2601

ABSTRACT

Si-doped n-type $Al_xGa_{1-x}N$ alloys with x up to 0.5 and Mg-doped p-type $Al_xGa_{1-x}N$ alloys with x up to 0.27 were grown by metal-organic chemical vapor deposition (MOCVD) on sapphire substrates. For the n-type $Al_xGa_{1-x}N$, we achieved highly conductive alloys for x up to 0.5. An electron concentration as high as 1 x 10^{18} cm^{-3} was obtained in Si-doped $Al_{0.5}Ga_{0.5}N$ alloys with an electron mobility of 16 cm^2/Vs at room temperature, as confirmed by Hall-effect measurements. Our results also revealed that (i) the conductivity of $Al_xGa_{1-x}N$ alloys continuously increases with an increase of Si doping level for a fixed value of Al content ($x < 0.5$), (ii) the conductivities of $Al_xGa_{1-x}N$ alloys decrease with increasing Al content for a given doping level; (iii) the critical Si-doping concentration needed to convert insulating $Al_xGa_{1-x}N$ with high Al contents ($x \geq 0.4$) to n-type conductivity is about 1 x 10^{18} cm^{-3}. Time-resolved photoluminescence studies carried out on these materials have shown that Si-doping reduces the effect of carrier localization in $Al_xGa_{1-x}N$ alloys and a sharp drop in carrier localization energy occurs when the Si doping concentration increases above 1 x 10^{18} cm^{-3}, which directly correlates with the observed electrical properties. For the Mg-doped $Al_xGa_{1-x}N$ alloys, p-type conduction was achieved for x up to 0.27, as confirmed by variable temperature Hall measurements. Emission lines of band-to-impurity transitions of free electrons with neutral Mg acceptors as well as localized excitons have been observed in the p-type $Al_xGa_{1-x}N$ alloys. The Mg acceptor activation energies E_A were deduced from photoluminescence spectra and were found to increase with Al content and agreed very well with those obtained by Hall measurements. From the measured activation energy as a function of Al content, E_A versus x, the resistivity of Mg-doped $Al_xGa_{1-x}N$ with high Al contents can be deduced. Our results have also shown that PL measurements provide direct means of obtaining E_A especially where this cannot be obtained accurately by electrical methods due to high resistance of p-type $Al_xGa_{1-x}N$ with high Al content.

Keywords: $Al_xGa_{1-x}N$, wide bandgap, time-resolved PL, optical transitions, UV light emitters

1. INTRODUCTION

There is currently a great need of solid-state ultraviolet (UV) emitters for detection of chemical and biological agents as well as for general lighting. In such applications based on III-nitride wide bandgap semiconductors, conductive n-type and p-type AlGaN alloys with high Al contents are indispensable. Improving the material quality of high Al content AlGaN alloys is also of crucial importance for fabricating high performance AlGaN/GaN heterojunction field effect transistors. In addition, highly conductive p-type films are necessary for improving the performances of laser diodes (LDs) including reducing their threshold voltages. However, n-type and p-type $Al_xGa_{1-x}N$ alloys with high x are both very difficult to grow and to characterize due to their wide energy band gaps. In particular, high p-type conductivity in $Al_xGa_{1-x}N$ alloys is difficult to achieve due to high activation energy of Mg dopants as well as reduced crystalline quality of the alloys. Recently, n-type conduction in $Al_{0.4}Ga_{0.6}N$ epilayers has been achieved by employing In-Si co-doping approach [1]. A few studies have been reported on Mg-doped p-type $Al_xGa_{1-x}N$ with low Al content ($x \leq 0.15$) [2-5]. It was found that the activation energies (E_A) of Mg acceptors in Mg-doped $Al_xGa_{1-x}N$ increased with increase in Al content. Because these materials are of great importance in realizing nitride-based optoelectronic devices, studies that could provide better understanding and realization of highly conductive n-type and p-type $Al_xGa_{1-x}N$ alloys with high x ($x \geq 0.4$) are urgently needed.

Here, we summarize our results on the growth and characterization of Si- doped n-type $Al_xGa_{1-x}N$ alloys with x up to 0.5 and Mg-doped p-type $Al_xGa_{1-x}N$ alloys with x up to 0.27. Our results revealed that (i) the conductivity of $Al_xGa_{1-x}N$ alloys continuously increases with an increase of Si doping level for a fixed value of Al content ($x < 0.5$), (ii) the conductivities of $Al_xGa_{1-x}N$ alloys decrease with increasing Al content for a given doping level; (iii) the critical Si-doping concentration needed to convert insulating $Al_xGa_{1-x}N$ with high Al contents ($x \geq 0.4$) to n-type conductivity is about 1 x 10^{18} cm^{-3}. For the Mg-doped $Al_xGa_{1-x}N$ alloys, p-type conduction was achieved for x up to 0.27. Photoluminescence (PL) emission lines due to band-to-impurity transitions of free electrons with neutral Mg acceptors as well as localized excitons have been observed in the p-type $Al_xGa_{1-x}N$ alloys. The Mg acceptor activation energies E_A were deduced from photoluminescence spectra and were found to increase with Al content and agreed very well with those obtained by Hall measurements.

Ultrafast Phenomena in Semiconductors VI, Kong-Thon F. Tsen, Jin-Joo Song, Hongxing Jiang, Editors, Proceedings of SPIE Vol. 4643 (2002) © 2002 SPIE · 0277-786X/02/$15.00

2. EXPERIMENT

Si-doped $Al_xGa_{1-x}N$ alloys of 1 μm thickness were grown by metal-organic chemical vapor deposition (MOCVD) on sapphire (0001) substrates with AlN buffer layers. The metal organic sources used were trimethylgallium (TMG) and trimethylaluminum (TMAl). For $Al_xGa_{1-x}N$ alloys with a fixed Al content ($0.3 \leq x \leq 0.5$), the doping level was varied from 0 to 5 x 10^{18} cm^{-3}. Mg-doped p-type $Al_xGa_{1-x}N$ epitaxial layers of 1 μm thickness were also grown by MOCVD on sapphire substrates with a 30 nm GaN buffer layers. For Mg doping, bis-cyclopentadienyl magnesium (Cp_2Mg) was transported into the growth chamber with ammonia during growth. Post-growth annealing at 950 °C in nitrogen gas ambient for 8 sec resulted in p-type conduction, verified by Hall measurements. The Al contents in these n-type and p-type $Al_xGa_{1-x}N$ alloys were determined by energy dispersive x-ray (EDX) microanalysis and x-ray diffraction (XRD) measurement as well as by the flow rates of TMG and TMAl. The Al contents (x) determined by all three methods agreed to within ± 0.02. The surfaces of the $Al_xGa_{1-x}N$ epilayers were examined using atomic force microscopy (AFM) and scanning electron microscopy (SEM) and were found to be crack-free. Variable temperature Hall-effect (standard Van der Pauw) measurements were employed to measure the electron concentration, mobility, and resistivity of these materials. A deep UV (10 mW @ 195 nm) picosecond time-resolved laser spectroscopy system was specially designed to probe the optical properties of materials and devices structures based on $Al_xGa_{1-x}N$ alloys with high x and hence serves as "eyes" for monitoring the qualities of these materials. The laser spectroscopy system basically consists of a frequency quadrupled 100 femtosecond Ti: sapphire laser with a 76 MHz repetition rate, a monochromator (1.3 m), and a streak camera with a detection capability ranging from 185 - 800 nm and a time resolution of 2 ps [6].

3. RESULTS AND DISCUSSIONS

3.1 High Al-content n-type AlGaN alloys

Table 1 summarizes the results from the room temperature Hall-effect measurement of the 25 $Al_xGa_{1-x}N$ samples. The general trends are that the conductivity of $Al_xGa_{1-x}N$ alloys increases with the Si doping level, N_{Si} (for a fixed value of x) and decreases with x (at a fixed value of N_{Si}). Free electron concentrations as high as 2.3 x 10^{18} cm^{-3} (with a mobility of 28 cm^2/Vs)

Table 1: Electrical data of Si-doped $Al_xGa_{1-x}N$

Conductivity ($[\Omega\text{-cm}]^{-1}$)
Mobility (cm^2/Vs) / Concentration (cm^{-3})

N_{si} (cm^{-3})	x = 0.3	x = 0.35	x = 0.4	x = 0.45	x = 0.5
0	7.32	0.47	$5.2x10^{-3}$	$2.6x10^{-3}$	
	12 / $3.81x10^{18}$	23 / $1.29x10^{17}$	8.6 / $3.81x10^{15}$	3.1 / $5.30x10^{15}$	High resistivity
$5.0x10^{17}$	0.4	0.49	0.16	0.21	0.23
	9.6 / $2.60x10^{17}$	11 / $2.80x10^{17}$	4.8 / $2.11x10^{17}$	4.9 / $2.3x10^{17}$	5.2 / $2.81x10^{17}$
$1.0x10^{18}$	0.62	4.5	0.67	0.13	0.013
	13 / $2.99x10^{17}$	36 / $7.82x10^{17}$	10 / $4.17x10^{17}$	4.2 / $1.92x10^{17}$	3.1 / $2.66x10^{16}$
$2.5x10^{18}$	15.3	21.0	15.4	4.85	**2.51**
	61 / $1.57x10^{18}$	56 / $2.35x10^{18}$	60 / $1.60x10^{18}$	37 / $8.19x10^{17}$	**16 / $9.82x10^{17}$**
$5.0x10^{18}$	25.7	34.2	10.0	**10.2**	0.88
	45 / $3.57x10^{18}$	62 / $3.45x10^{18}$	19 / $3.16x10^{18}$	**28 / $2.28x10^{18}$**	14 / $3.94x10^{17}$

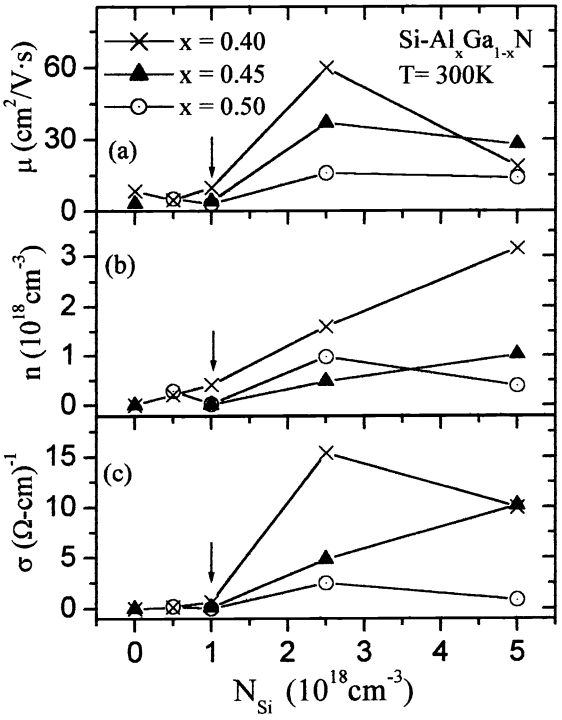

Fig. 1. (a) Mobility μ, (b) electron concentration n and (c) conductivity σ of Si-doped $Al_xGa_{1-x}N$ alloys as a function of Si doping concentration N_{si} for three different Al compositions x = 0.4, 0.45 and 0.5.

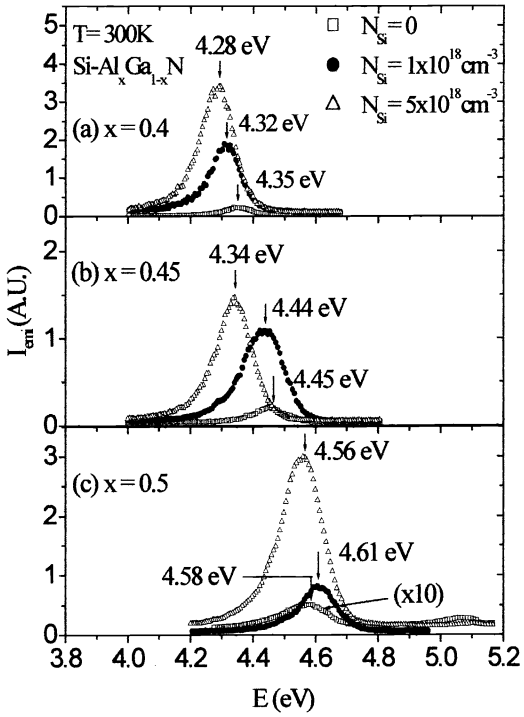

Fig. 2. Room temperature PL spectra of Si-doped $Al_xGa_{1-x}N$ alloys with three different doping concentrations for (a) x = 0.4, (b) x = 0.45 and (c) x = 0.5.

and 1x 10^{18} cm^{-3} (with a mobility of 16 cm^2/Vs) have been achieved in $Al_{0.45}Ga_{0.55}N$ and $Al_{0.5}Ga_{0.5}N$ alloys, respectively. The data shown in Table 1 are plotted in Fig. 1 for representative samples (of x = 0.4, 0.45, and 0.5), showing variation of electron mobility, electron concentration, and conductivity of Si-doped $Al_xGa_{1-x}N$ alloys with Si doping concentrations N_{Si}. We see that the electron concentration, mobility, and conductivity all increase with increasing N_{Si}. However, the enhancements in electron concentration, mobility, and conductivity due to Si doping decrease with increasing x. In particular for x = 0.5, there appears to be a limit on the degree of improvement on the electrical property by Si doping, i.e., the conductivity of $Al_{0.5}Ga_{0.5}N$ alloys has a maximum at N_{Si} = 2.5 x 10^{18} cm^{-3} instead of at N_{Si} = 5 x 10^{18} cm^{-3}. An important result shown in Fig. 1 is that there exists a critical Si-doping concentration of about 1 x 10^{18} cm^{-3} for converting insulating $Al_xGa_{1-x}N$ with high Al contents (x ≥ 0.4) to n-type conductivity. We believe that this is a direct consequence of electrons filling the localized states in $Al_{0.5}Ga_{0.5}N$ alloys caused by alloy fluctuation. Our results here suggest that below the mobility edge (energy that separates the localized states from the extended states), the density of the localized states in $Al_xGa_{1-x}N$ alloys with x ≥ 0.4 is on the order of 1 x 10^{18} cm^{-3}.

Fig. 2 shows room-temperature (300 K) PL spectra of $Al_xGa_{1-x}N$ with three different Si doping concentrations (N_{Si}) at fixed Al content x = 0.4, 0.45, and 0.5. In addition to the shift of the peak positions (E_p) toward longer wavelengths at higher doping levels due to the effect of the bandgap renormalization, we also observe a considerable increase in the PL emission intensity with increasing N_{Si}. The improvement of optical quality by Si doping has been observed previously in GaN epilayers [7-9] and AlGaN/GaN multiple quantum wells [10]. The relative PL intensities for Si-doped $Al_xGa_{1-x}N$ alloys seen here increase by about one order of magnitude when the Si doping concentration is varied from 0 to 5 x 10^{18} cm^{-3}. For example, for x = 0.45, the relative PL emission intensity increases from 5 to 37 and to 44 as the doping concentration increases from 0 to 1 x 10^{18} cm^{-3} and to 5 x 10^{18} cm^{-3}.

To investigate the influence of the Si doping concentration on the carrier localization properties of the $Al_xGa_{1-x}N$ alloys, we measured the carrier localization energy and recombination lifetime as functions of Si doping for representative samples. Fig. 3 shows the Arrhenius plots of PL intensity for n-type $Al_{0.45}Ga_{0.55}N$ epilayers with different Si doping levels up to 5 x 10^{18} cm^{-3}. The solid lines in Fig. 3 are the least squares fit of data with equation

$$I_{emi}(T) = I_0/[1 + C\exp(-E_0/kT)] \quad (1)$$

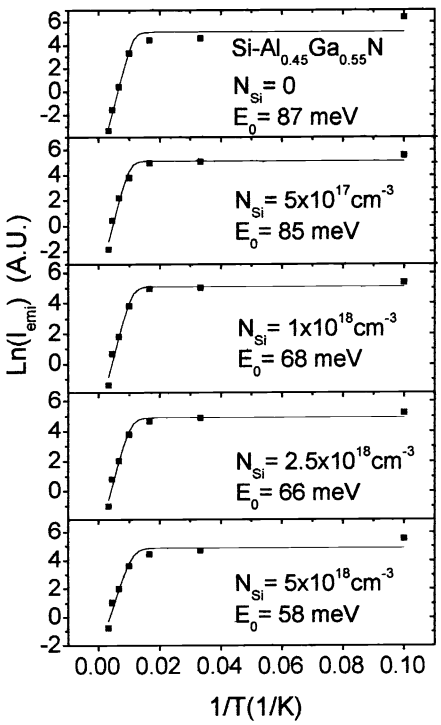

Fig. 3. The Arrhenius plots of integrated PL intensity for Si-doped $Al_{0.45}Ga_{0.55}N$ alloys with different Si doping concentration N_{si} ranging from 0 to 5 x 10^{18} cm^{-3}. The solid lines are the least square fit of the data with Eq. (1).

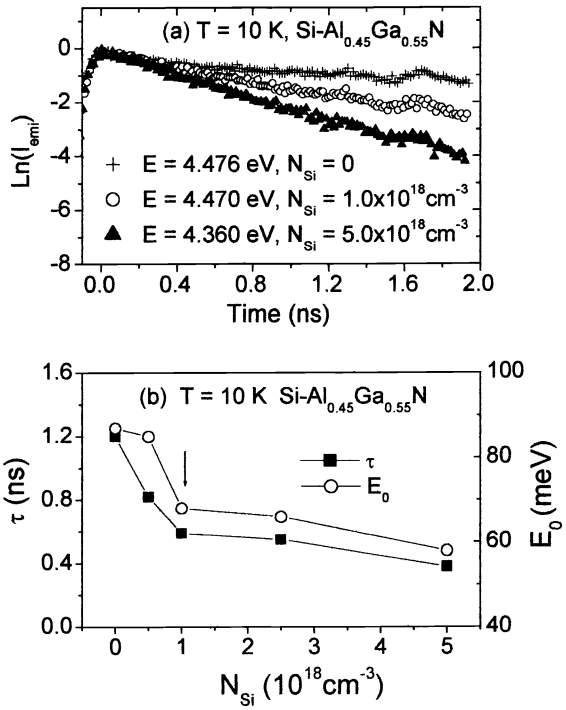

Fig. 4. (a) Time resolved PL emission measured at 10K for Si-doped $Al_{0.45}Ga_{0.55}N$ alloys with three different Si doping concentrations. (b) Si-doping concentration dependence of measured decay time and activation energy E_o of Si-doped $Al_xGa_{1-x}N$ alloys.

where E_0 is the activation energy of the PL emission, which is a measure of the carrier localization energy. The fitted activation energies E_o are also indicated in Fig. 3. Time-resolved PL was employed to measure the carrier recombination lifetimes at different doping levels. Fig. 4(a) shows temporal responses of PL emission of Si doped $Al_{0.45}Ga_{0.55}N$ samples with three different doping concentrations measured at their respective spectral peak positions. It clearly shows a systematic decrease of the recombination lifetime with increasing N_{Si}. The recombination lifetime τ and activation energy E_0 of PL emission for Si-doped $Al_{0.45}Ga_{0.55}N$ epilayers as functions of doping level are plotted in Fig. 4(b). Both values of τ and E_0 exhibit initial sharp decreases when the Si doping concentration is increased from $N_{Si} = 0$ to $N_{Si} = 1 \times 10^{18}$ cm^{-3}, followed by gradual decreases as N_{Si} is further increased. These results suggest that Si-doping reduces the carrier localization effect with a sharp reduction in carrier localization energy taking place at around $N_{Si} = 1 \times 10^{18}$ cm^{-3}. The results shown in Fig. 4(b) thus corroborate the electrical data presented in Table 1 and in Fig. 1. Our results suggest that the critical Si-doping concentration needed to fill up the localized states in $Al_xGa_{1-x}N$ alloys ($x \geq 0.4$) is around $N_{Si} = 1 \times 10^{18}$ cm^{-3}, above which carriers are able to transport via extended states and reasonable conductivities can be achieved. Therefore in order to obtain good n-type conductivities in $Al_xGa_{1-x}N$ alloys ($x \geq 0.4$), Si doping levels above 1 x 10^{18} cm^{-3} is required.

3.2 High Al-content p-type AlGaN alloys

Fig. 5 shows the room temperature (300 K) cw PL spectra of the Mg-doped p-type $Al_xGa_{1-x}N$ for x = 0.22 after anneal of 950 °C for 8 sec and two emission peaks at 3.2 eV and 3.62 eV are observed. The emission peak at 3.2 eV is the main peak and in some of the samples studied, this was the only peak observed. The 3.2 eV transition has been well documented in Mg-doped p-type GaN, which is located at 2.95 eV [11]. A further anneal at 600 °C for 2 min in nitrogen gas resulted in the spectrum shown in Fig. 5 (b) where the peak at 3.2 eV is now reduced significantly at room temperature. The peak at 3.62 eV is slightly red-shifted to 3.60 eV but is now predominant, with about an order of increase in the emission intensity.

Fig. 6 shows room temperature (300 K) cw PL spectra of the Mg-doped p-type $Al_xGa_{1-x}N$ for x = 0.22, 0.25 and 0.27,

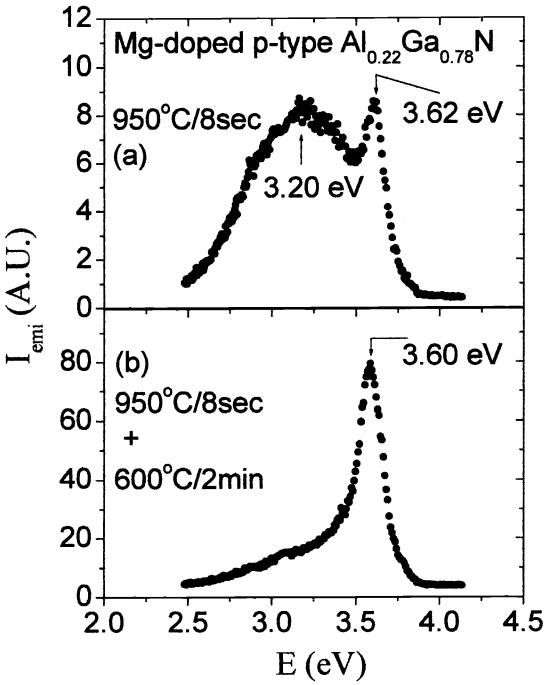

Fig. 5. Room temperature (300 K) cw-PL spectra of the Mg-doped p-type $Al_{0.22}Ga_{0.78}N$ (a) after anneal of 950°C for 8 s (b) after a second anneal at 600°C for 2 min.

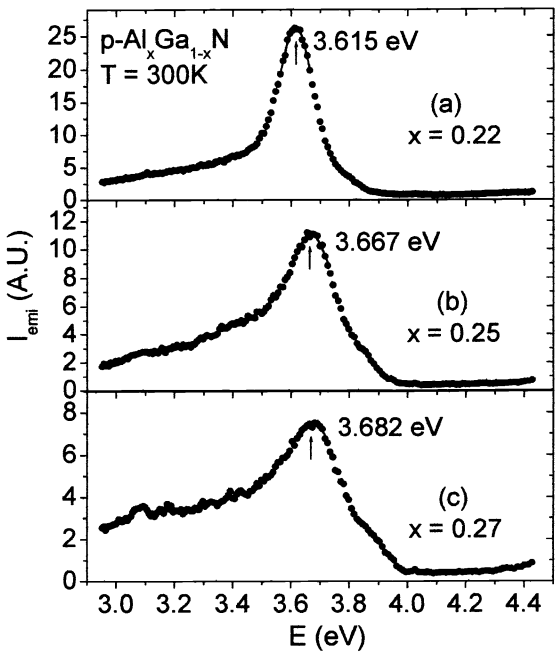

FIG. 6. Room temperature (300 K) cw PL spectra from Mg-doped p-type $Al_xGa_{1-x}N$ for (a) x = 0.22, (b) x = 0.25 and (c) x = 0.27.

following the two-step anneals described above. As can be seen, the emission intensities of these spectra decrease with increase in x, a phenomenon we observed previously [12] which is related to reduction in crystalline quality with increasing x. The emission peaks are observed at 3.615 eV, 3.667 eV and 3.682 eV for x = 0.22, 0.25 and 0.27 respectively, which are greater than the band edge transition of 3.42 eV for GaN. We assign these emission lines to the band-to-impurity transitions for the recombination of free electrons with neutral Mg acceptors in $Al_xGa_{1-x}N$. With the origin of these peaks thus assigned, the activation energy $E_A(x)$ of the ionized Mg impurity in $Al_xGa_{1-x}N$ can be deduced simply by the difference between the energy gap E_g (x) and the observed band-to impurity emission peak $E(e^-, A^o)$. E_g (x) can be estimated from the expression

$$E_g(x) = (1-x)E_{g,GaN} + xE_{g,AlN} - bx(1-x) \qquad (2)$$

and $E_A(x) = E_g(x) - E(e^-, A^o)$. In the above expression, we used widely accepted value of the energy gap for GaN, $E_{g,GaN}$ = 3.42 eV, for AlN, $E_{g,AlN}$ = 6.20 eV and of the bowing parameter b = 0.90 [13]. With these, E_A values of 0.262 eV, 0.279 eV and 0.311 eV corresponding to Al contents 0.22, 0.25 and 0.27, respectively, are obtained. It is expected that different choices of the bowing parameter b would result in variations in the E_A values. However, because the Mg acceptor level in AlGaN alloys is quite deep, the uncertainties in the E_A values due to different choices of b are not very significant. For example, the above optically obtained E_A values from Eq. (2) will be reduced by about 17 - 20 meV if the bowing parameter b = 1 is used.

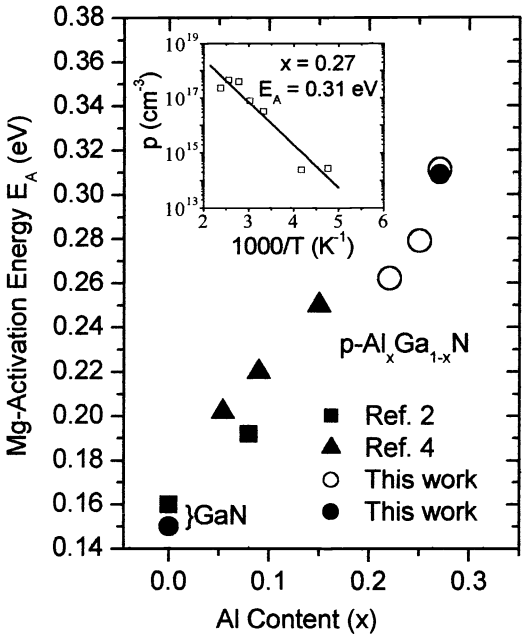

FIG. 7. Activation energies of Mg acceptors in Mg-doped p-type $Al_xGa_{1-x}N$ as a function of Al content x. Closed squares and triangles are data from ref. 2 and 4 respectively, while closed circles are data from this work, all obtained by Hall measurements. Open circles indicate data obtained by PL measurements from this work. The inset shows measured temperature dependence of Hall concentration (p) in the Mg-doped p-type $Al_{0.27}Ga_{0.73}N$ sample from which E_A = 0.310 eV was obtained.

The values of E_A we obtained in the above manner are plotted as a function of Al content x in Fig. 7, together with those reported previously [2, 4], all obtained by means of variable temperature Hall measurements. Also shown in this figure are data points for p-GaN and for p-$Al_{0.27}Ga_{0.73}N$ where we determined E_A by variable temperature Hall measurements (0.15 eV and 0.309 eV respectively). The measured temperature dependence of Hall concentration (p) in the Mg-doped p-type $Al_{0.27}Ga_{0.73}N$ sample is shown in the inset of Fig. 7, from which a value E_A = 0.310 eV was obtained. Since the hole concentrations in AlGaN alloys are relatively low and impurity band formation is not likely, our results of E_A deduced from the PL spectra match quite well with those obtained by Hall measurements, which further corroborates our assignment that the observed transitions between 3.62 - 3.68 eV in Fig. 6 are band-to-impurity transitions of free electrons to the neutral Mg acceptors. The increase of E_A with increase in band gap energy for the III-nitrides has been reported previously in other studies [2, 4, 14] and is predicted by the effective mass theory [15-17]. As a comparison with our results, the value of E_A estimated from the effective mass theory for x = 0.25 for example, is between 0.263 and 0.294 eV which agrees with the measured value of 0.279 eV.

Fig. 8 shows low temperature (10 K) cw PL spectrum of one of the samples with x = 0.22, where three emission peaks at 3.327 eV, 3.623 eV and 3.823 eV were resolved. The peak observed at 3.623 eV is the same transition of free electrons to the neutral Mg acceptors, which was observed at 3.615 eV at 300K [Fig. 6 (a)]. The peak at 3.823 eV is believed to be due to the recombination of localized excitons, with the peak energy E_p given by

$$E_p = E_g - E_{bx} - E_{loc} \tag{3}$$

where E_g is the energy gap as defined in Eq. (2), E_{bx} is the excitonic binding energy and E_{loc} is the localization energy of the localized exciton. For x = 0.22, the value E_g = 3.877 eV is obtained from Eq. (2). With estimated values of E_{bx} = 25 meV and E_{loc} = 30 meV [12], a value of E_p = 3.822 eV is obtained for x = 0.22, which matches quite well with the observed emission peak (3.823 eV) in this spectrum, supporting our assignment of localized exciton for this emission line.

The dynamics of the optical transitions in the Mg-doped p-type $Al_xGa_{1-x}N$ was investigated by measuring the PL temporal response of one sample with x = 0.22 at 10 K. The data for the transient measurements at emission peaks 3.327 eV and

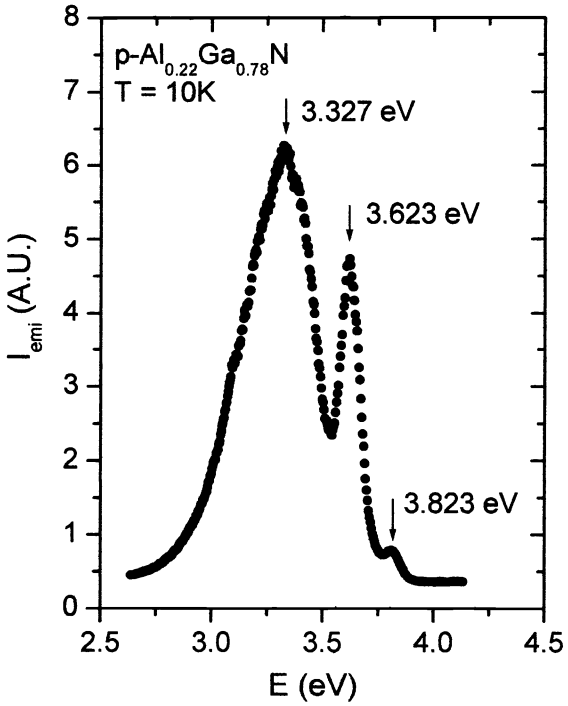

FIG. 8. Low temperature (10 K) cw PL spectrum of Mg-doped p-type $Al_xGa_{1-x}N$ with x = 0.22.

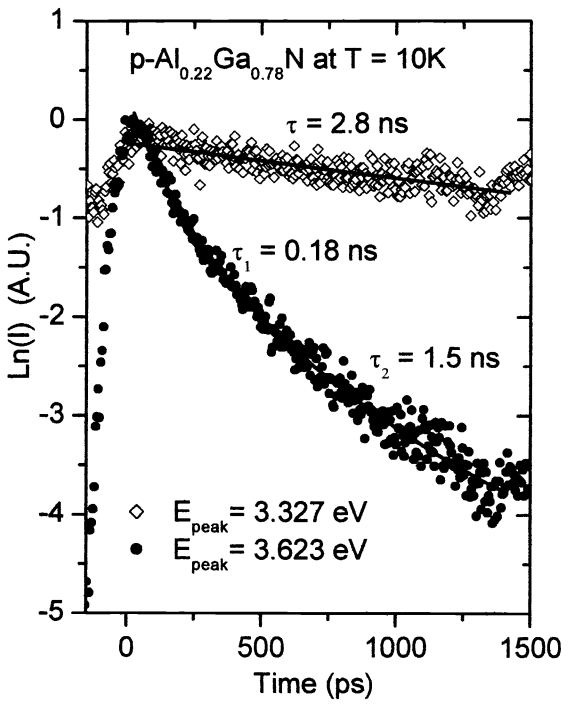

FIG. 9. Temporal response of the PL emissions from Mg-doped p-type $Al_{0.22}Ga_{0.78}N$ at 3.327 eV and 3.623 eV. The decay at 3.327 eV can be fitted with a single exponential giving a lifetime of 2.8 ns, while that at 3.623 eV can be fitted with two exponentials, with lifetimes of 0.18 ns and 1.5 ns. Continuous lines are fittings to the data points.

3.623 eV are shown in Fig. 9. The decay at 3.327 eV can be fitted quite well with a single exponential giving a lifetime of 2.8 ns, while that at 3.623 eV can be fitted with two exponentials, with lifetimes of 0.18 ns and 1.5 ns. The difference in the decay dynamics of these two peaks is an indication that the origin of the 3.327 eV line is quite different from that of the 3.623 eV line. The orders of the measured decay lifetimes of the 3.623 eV line are consistent with the assigned optical transitions described above.

From the measured E_A versus x in Mg-doped p-type $Al_xGa_{1-x}N$, the resistivity versus x can be estimated as follows:

$$\rho(Al_xGa_{1-x}N) = \rho_o \exp(E_A/kT) = \rho_o \exp\{[E_A(GaN) + \Delta E_A]/kT\} = \rho(GaN)\{\exp(\Delta E_A]/kT)\} \quad (4)$$

where $\Delta E_A = E_A(Al_xGa_{1-x}N) - E_A(GaN)$ and our typical p-type GaN has resistivity of about 1.0 Ω-cm. From Eq. (4), the resistivity of $Al_xGa_{1-x}N$ alloys with higher values of x can be deduced. For example, if the trend in Fig. 7 holds for higher x, at Al content x = 0.45, the activation energy E_A is estimated to be 0.4 eV and the estimated resistivity should be as high as 2.2×10^4 Ω-cm. Our results thus indicate that alternative methods for acceptor activation in AlGaN alloys with high Al contents have to be developed. The exponential increase of the resistivity with ΔE_A implies that the Hall measurements can no longer be used to measure the activation energy of $Al_xGa_{1-x}N$ alloys with high Al contents where the resistivity becomes very high. However with the observation of band-to-impurity transition, the PL method would be the alternative method for the determination of Mg acceptor activation energy.

4. SUMMARY

In summary, we have investigated the growth, optical, and electrical properties of Si-doped $Al_xGa_{1-x}N$ alloys with x up to 0.5 and of Mg-doped $Al_xGa_{1-x}N$ with x up to 0.27. Our results revealed that (i) the conductivity of Si-doped n-type $Al_xGa_{1-x}N$ alloys increases with the Si doping level (N_{Si}) and a sharp increase occurs around $N_{Si} = 1 \times 10^{18}$ cm^{-3} due to the filling of localized states by electrons; and (ii) high conductivity can be achieved for x up to 0.5 by Si doping. We have also obtained p-type conductivity in Mg-doped $Al_xGa_{1-x}N$ for x up to 0.27. The PL spectra show band-to-impurity transitions of free electrons with neutral Mg acceptors in the $Al_xGa_{1-x}N$. The values of activation energy E_A of the ionized Mg impurity in $Al_xGa_{1-x}N$ deduced from these spectra match quite well with those obtained by Hall measurements and increase with an increase of Al content, as predicted by the effective mass theory. However, further improvement in the conductivities of $Al_xGa_{1-x}N$ alloys with higher x is still needed.

ACKNOWLEDGEMENTS

This research is supported by grants from DARPA, BMDO, ARO, ONR, DOE (96ER45604/A000), and NSF (DMR-9902431 and INT-9729582).

REFERENCES

a) Electronic mail: jiang@phys.ksu.edu

1. V. Adivarahan, G. Simin, G. Tamulaitis, R. Srinivasan, J. Yang, and M. Asif Khan, *Appl. Phys. Lett.* **79**, 1903 (2001)
2. T. Tanaka, A. Watanabe, H. Amano, Y. Kobayashi, I. Akasaki, S. Yamazaki and M. Koike, *Appl. Phys. Lett.* **65**, 593 (1994).
3. I. Akasaki and H. Amano, Mater. Res. Soc. Symp. Proc. **242**, 383 (1991).
4. M. Suzuki, J. Nishio, M. Onomura and C. Hongo, *J. Cryst. Growth* **189/190**, 511 (1998).
5. L. Sugiura, M. Suzuki, J. Nishio, K. Itaya, Y. Kokubun, and M. Ishikawa, *Jpn. J. Appl. Phys. Part 1* **7**, 3878 (1998).
6. http://www.phys.ksu.edu/area/GaNgroup.
7. Xiong Zhang, Soo-Jin Chua, Wei Liu, and Kok-Boon Chong, *Appl. Phys. Lett.* **72**, 1890 (1998).
8. Z. Q. Li, H. Chen, H. F. Liu, L. Wan, M. H. Zhang, Q. Juang, and J. M. Zhou, *Appl. Phys. Lett.* **76**, 3765 (2000).
9. S. Ruvimov, Z. Liliental-Weber, T. Suski, J. W. Ager III, and J. Washbum, *Appl. Phys. Lett.* ***69***, 990 (1996).

10. K. C. Zeng, J. Y. Lin, H. X. Jiang, A. Salvador, G. Popovici, H. Tang, W. Kim, and H. Morkoc, *Appl. Phys. Lett.* **71**, 1368 (1997).
11. M. Smith, G. D. Chen, J. Y. Lin, H. X. Jiang, A. Salvador, B. N. Sverdlov, A. Botchkarev, H. Morkoc and B. Goldenberg, *Appl. Phys. Lett.* **68**, 1883 (1996).
12. H. S. Kim, R. A. Mair, J. Li, J. Y. Lin and H. X. Jiang, *Appl. Phys. Lett.* **76**, 1252 (2000).
13. Y. Koide, H. Itoh, M. R. H. Khan, K. Hiramato, N. Sawaki and I. Akasaki, *J. Appl. Phys.* **61**, 4540 (1987).
14. K. Kumakura, T. Makimoto and N. Kobayashi, *Jpn. J. Appl. Phys.* **39**, L337 (2000).
15. I. Akasaki and H. Amano, *Jpn. J. Appl. Phys.* **36**, 5393 (1997).
16. J. B. Xia, K. W. Cheah, X. L. Wang, D. Z. Sun and M. Y. Kong, Phys. Rev. B **59**, 10119 (1999).
17. F. Mireles and S. E. Ulloa, Phys. Rev. B **58**, 3879 (1998).